Universität Karlsruhe (TH)
Forschungsuniversität • gegründet 1825

Institut für Mechanik

Thermal Stresses in Ceramometallic Crowns: Firing in Layers

J. Lenz, M. Thies, Karl Schweizerhof
Universität Karlsruhe, Institut für Mechanik
Q. Rong
Peking University, Department of Mechanics and Engineering Science

2002

Institut für Mechanik
Kaiserstr. 12, Geb. 20.30
76128 Karlsruhe
Tel.: +49 (0) 721/ 608-2071
Fax: +49 (0) 721/ 608-7990
E-Mail: ifm@uni-karlsruhe.de
www.ifm.uni-karlsruhe.de

Thermal Stresses in Ceramometallic Crowns: Firing in Layers

Juergen LENZ, Dr Rer Nat*, Matthias THIES, Dr-Ing**,
Karl SCHWEIZERHOF, Dr-Ing***, Qiguo RONG, MSc****

Objective: *This investigation deals with the experimental/numerical determination of transient and residual thermal stresses in ceramometallic crowns, simulating a realistic case of firing in (four) layers.*
Methods: *Axisymmetric (premolar) crown models with a NiCr-frame were equipped with thermocouples on the outer and inner surfaces. The crowns were heated in a porcelain furnace to a homogeneous temperature of 600 °C in each simulated firing step. After opening the lid of the furnace, the temperature decreases in the different surface points when measured simultaneously throughout the cooling phase. From these data the temperature and stress distributions in the crown were computed with the aid of the Finite Element Method, assuming linear-thermoelastic behavior of alloy and porcelain and taking into account the dependence of the porcelain's coefficient of thermal expansion on the number of firings.*
Results: *For the porcelain employed maximum transient thermal stresses in the veneer occurred during the firing of opaque ceramic shortly after opening the furnace. In each further firing step the maximum transient stresses were reduced. Maximum residual stresses were found after the second firing of the body porcelain. Glazing led to a considerable relief of the transient thermal stresses.*
Conclusion: *The results allow a deeper understanding of the origins of thermal stresses during the fabrication process of ceramometallic crowns and of the influence of several decisive fabrication parameters on the magnitude of theses stresses. In view of the large number of parameters involved, it must be questioned whether a satisfactory definition of "thermal compatibility" of alloy and ceramic can ever be established.*
Key words: *Porcelain-fused-to-metal (PFM) restorations, ceramometallic premolar crown, transient and residual thermal stresses, thermal compatibility, temperature measurement, Finite Element Method (FEM).*

Porcelain-fused-to-metal (PFM) restorations (crowns, bridges, prostheses) are fabricated by coating an alloy frame with ceramic in several steps, heating the system each time in a porcelain furnace to temperatures of $\vartheta \approx (930–980)$ °C, and cooling it (according to a given timescale) first inside and later outside the furnace. Generally four firings are necessary for the completion of the restoration:

1. *Opaque porcelain firing* whereby the opaque ceramic prevents a translucence of the alloy frame and brings about a sufficiently high bond between the porcelain and the frame;
2. *First dentin (body porcelain) firing;*
3. *Second dentin firing* in order to make up for the volume loss in the preceding cycle and thus achieve the final geometry of the restoration (otherwise at least one further firing is necessary);
4. *Glazing* in order to seal possible microcracks in the surface of the veneer and endow it with the gloss of a natural tooth.

* Academic Director, Centre for Scientific Computing and Mathematical Modelling, University of Karlsruhe, Karlsruhe, Germany.
** Research Assistant, Institute for Mechanics, University of Karlsruhe, Karlsruhe, Germany.
*** Professor, Institute for Mechanics, University of Karlsruhe, Karlsruhe, Germany.
*** Research Assistant, Department of Mechanics and Engineering Science, Peking University, Beijing, PR China.
Reprint requests: Dr Juergen LENZ, Centre for Scientific Computing and Mathematical Modelling, University of Karlsruhe, D - 76128 Karlsruhe, Germany. Telephone: ++49 721 608 2613; Fax: ++49 721 608 7990; E-mail: Juergen.Lenz@math.uni-karlsruhe.de.
This work was financially supported by the Deutsche Forschungsgemeinschaft (SCHW 307/5-1, 5-2, 5-3).

During the cooling phase after each firing, when passing through its so-called glass-transformation temperature interval which is in the range of $\vartheta_G \approx$ (560–620) °C for the majority of conventional porcelains, ceramic changes from a plastic-sluggish into an elastic-brittle state. While at temperatures of $\vartheta > \vartheta_G$ the porcelain can follow the contraction of the frame without experiencing stresses; at temperatures of $\vartheta < \vartheta_G$ thermal stresses build up in the composite system since the coefficient of thermal expansion, α, of the now elastic-stiff ceramic differs from that of the alloy during the cooling to room temperature. If the frame and veneer could contract freely, they would no longer fit together, but since they are connected along the bond surface constraints arise in the system. In "thermally-incompatible" material combinations (with too large a difference in the coefficients of thermal expansion as an essential criterion) critical thermal stresses lead to cracks and/or spallations in the veneer or to debonding. An increase in such defects is commonly observed when dental technicians change over to a new alloy and/or porcelain. Therefore, it is helpful to analyze the development of thermal stresses and study their dependence on the essential parameters.

In the following study we restrict ourselves to the investigation of thermal stresses in PFM *crowns,* selecting an *axisymmetric* crown model for reasons which will be explained. In particular we consider a model resembling a *premolar crown* in size (height and maximum radius), geometry of cusp and margin, and thickness of frame and ceramic veneer.

The analysis was carried out with the aid of the Finite Element Method (FEM). Besides the so-called *residual* stresses, i.e. thermal eigenstresses in the configuration at room temperature, we also analyzed the *transient* stresses, i.e. stresses occurring during the complete cooling phase.

Mathematically the temperature distribution in the *complete* crown as a function of time is given if the *initial* temperature distribution in the *complete* crown and either the heat flux from the crown into the vicinity, or the temperature distribution at its *surface* (both as functions of time) are known. The heat flux is caused by radiation and by free convection. Although the physical laws behind these phenomena are known, because of the complex geometry of the system they can not be realistically simulated by a numerical procedure. We therefore decided to determine the *surface* temperature *experimentally* by equipping the surfaces of the frame and of the veneer with thermocouples.

Two effects contribute to thermal stresses in a ceramometallic crown:

1) In an infinitely slow cooling of the system, which would result in a *homogeneous* temperature in the crown at each instant, where the frame and the veneer could contract freely, below the glasstransformation temperature they would no longer fit together because of the different rates of contraction of the two materials. However, since both parts are connected at the bond interface, constraints and thus stresses arise.
2) In reality, however, the crown is cooled in a finite period. Since the heat fluxes (due to radiation and convection) from the frame and the veneer into the vicinity differ from each other, position- and time-dependent temperature gradients (*inhomogeneous* temperature distributions as a function of cooling time) build up in the crown during cooling which also lead to thermal stresses. Because of the comparatively high thermal conductivity of the alloy, temperature differences within the frame will rapidly even out so that the temperature gradients and accompanying thermal stresses will essentially be limited to the veneer, i.e. to that part of the crown which is most vulnerable.

Even if it were possible identically to match the thermal contraction curves of an alloy and a porcelain throughout the period between the glass-transformation temperature of the ceramic and room temperature, although the cooled-down crown would certainly be free of stresses, during the cooling phase thermal stresses would still occur because of temperature gradients.

Indeed, the problem is rather intricate. The *residual* stresses depend only on the (mean) coefficients of thermal expansion, α_M and α_C, in the interval between the glass-transformation temperature of the porcelain, ϑ_G, and room temperature, ϑ_R, the glass-transformation temperature itself, Young's moduli, E_M and E_C, and Poisson's ratios, ν_M and ν_C, each at room temperature (M: metal, C: ceramic), and global and local geometry. The *transient* thermal stresses, however, are essentially affected by the specific cooling *history,* and the computation of the development of temperature and stresses requires the *temperature dependence* of all these material coefficients as well as of the mass densities, ρ_M and ρ_C, thermal conductivities, λM and λC, and specific heats, c_M and c_C. In view of this large number of parameters (and more, cf. our earlier studies[1,2]) it is questionable whether a satisfactory definition of the "thermal compatibility" of alloy and ceramic can ever be achieved.

In our first study[1] transient and residual thermal stresses in the geometrically identical premolar PFM crown model, as used here, were calculated for a simpli-

fied case in which the ceramic veneer was fixed to the alloy frame in one firing. The main result was that for all four tested alloys (gold, palladium, NiCr and the CoCr group) in combination with ips-Classic porcelain (Ivoclar, Liechtenstein), the maximum transient thermal stresses occurring shortly after opening the furnace considerably exceeded the maximum residual stresses in the crown's veneer. In practice, however, porcelain is fused to the alloy frame in several steps. In this study we therefore concentrate on an analysis of stresses caused by firing the ceramic veneer to the metal frame in three steps, followed by glazing. This analysis takes into account the temperature dependence of all the material coefficients involved, and in particular considers the dependence of the coefficients of thermal expansion of both, opaque and body porcelain, on the number of firings.

Alloy and porcelain are treated here as homogeneous, isotropic, linear-elastic materials, thus obeying the constitutive relations

$$\sigma(\varepsilon,\vartheta) = 2G \{ \varepsilon + [\nu e - (1+\nu)\,\alpha\,(\vartheta - \vartheta_G)]\,\mathbf{1} / (1-2\nu) \}$$

where σ = stress tensor, ε = deformation tensor, $\mathbf{1}$ = unit tensor, e = (volume) dilatation, ϑ = (instantaneous) temperature, ϑ_G = glass-transformation temperature of the porcelain, G = shear modulus, ν = Poisson's ratio [Young's modulus is given by $E = 2G\,(1 + \nu)$], and α = coefficient of thermal expansion. For the determination of *transient* thermal stresses the mass density, ρ, thermal conductivity, λ, and specific heat, c, of the materials are also involved as they appear in Fourier's equation of heat conduction. We disregard viscoelastic effects, however, which can not be excluded for porcelain, especially at temperatures around its glass-transformation temperature.[3,4] The presented stress values are therefore likely to be somewhat higher than those in a real crown. This does not, however, impair the comparison of stress distributions in the various firing cycles which is subsequently presented.

Materials and Methods

1. Materials

For the crown's frame the NiCr-alloy Williams Litecast (manufacturer: Williams, Amherst, NY) was used (composition: Ni 68.5 , Cr 15.5 , Mo 14.0 , Al 1.0 , Si , Mn). As veneering material ips-Classic porcelain (manufacturer: Ivoclar, Liechtenstein) was chosen. Table 1 presents the values of those material coefficients which determine the *residual* thermal stresses. They were partly provided by the manufacturers, partly taken from literature.[5,6]

For the determination of *transient* thermal stresses a knowledge of the temperature-dependence of all material coefficients is required. Figs 1 and 2 show the coefficients of thermal expansion, α, of opaque and body porcelain, and the NiCr-alloy, respectively, for the different firings as a function of temperature (the corresponding measurements of thermal strain were provided by Ivoclar, Liechtenstein). The temperature dependencies of the Young's moduli, E, Poisson's ratios, ν, thermal conductivities, λ, and specific heat capacities, ρc, as used in the calculations, are presented in Figs 3-6. These figures also include, for comparison, the temperature lapses of an AuPt-alloy (Aquarius C; manufacturer: Williams, Ellwangen, Germany), a PdAg-alloy (Capricorn Aries; manufacturer: Williams, Ellwangen, Ger-

TABLE 1 Young's modulus and Poisson's ratio at room temperature ϑ_R = 20 °C, glass-transformation temperatures, and coefficients of thermal expansion in the interval $\vartheta_R - \vartheta_G$

	Young's modulus E [GPa] (at ϑ_R)	Poisson's ratio ν (at ϑ_R)	Glass-transformation temperature ϑ_G [°C]			Coefficient of thermal expansion in the interval $\vartheta_R - \vartheta_G$ α [10^{-6} K^{-1}]		
Williams Litecast	158.6	0.27					14.4	
ips-Classic porcelain	69.4	0.19		opaque	body		opaque	body
			1st firing:	601.1	575.4	1st firing:	12.5	13.2
			2nd firing:	611.6	585.2	2nd firing:	11.2	12.1
			3rd firing:	618.1	580.9	3rd firing:	12.1	12.6
			4th firing:	610.6		4th firing:	12.5	

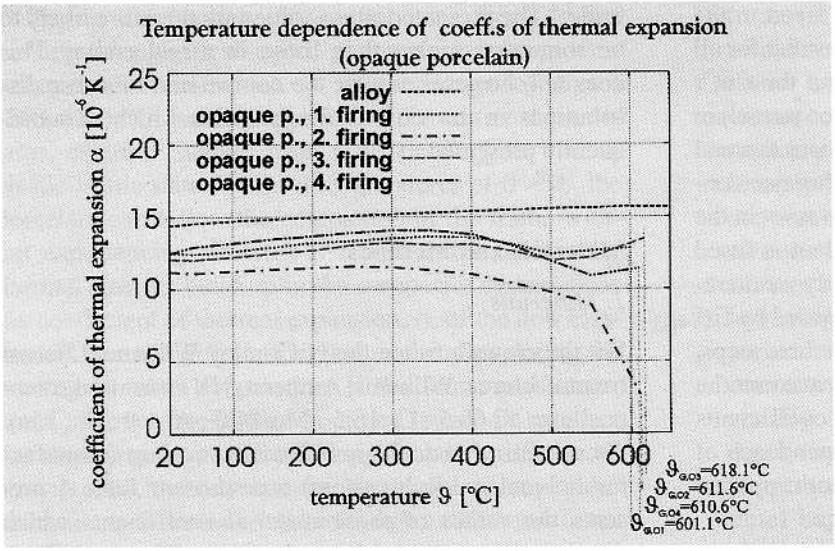

Fig 1 Coefficient of thermal expansion of opaque porcelain, and of NiCr-alloy, for the different firings as a function of temperature (including glass-transformation temperatures).

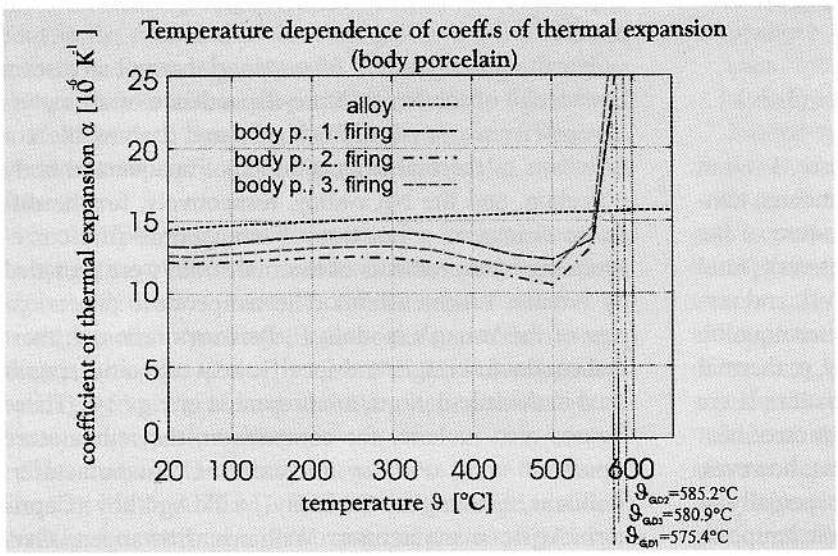

Fig 2 Coefficient of thermal expansion of body (dentin) porcelain, and of NiCr-alloy, for the different firings as a function of temperature (including glass-transformation temperatures).

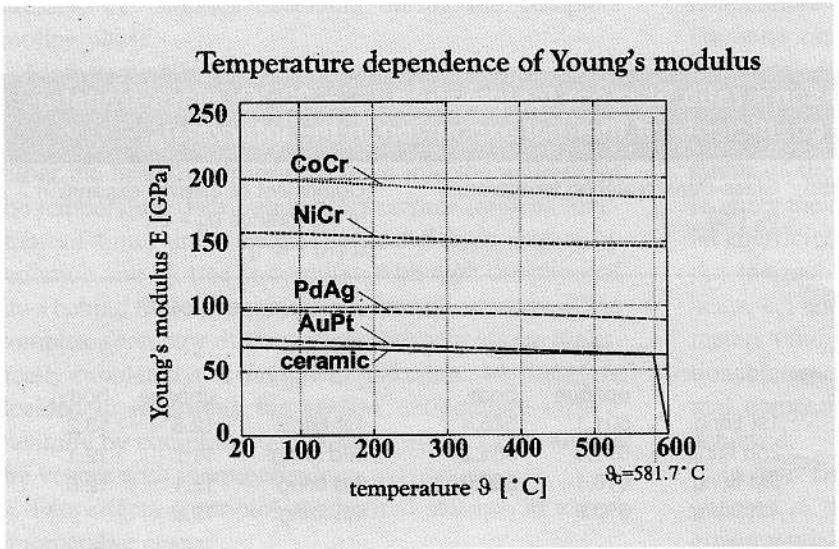

Fig 3 Temperature-dependence of Young's moduli of different alloys, and of porcelain. In the simulation of the different firing cycles the descent of the value of the porcelain near the glass-transformation temperature was chosen in the manner illustrated here for ϑ_G = 581.7 °C.

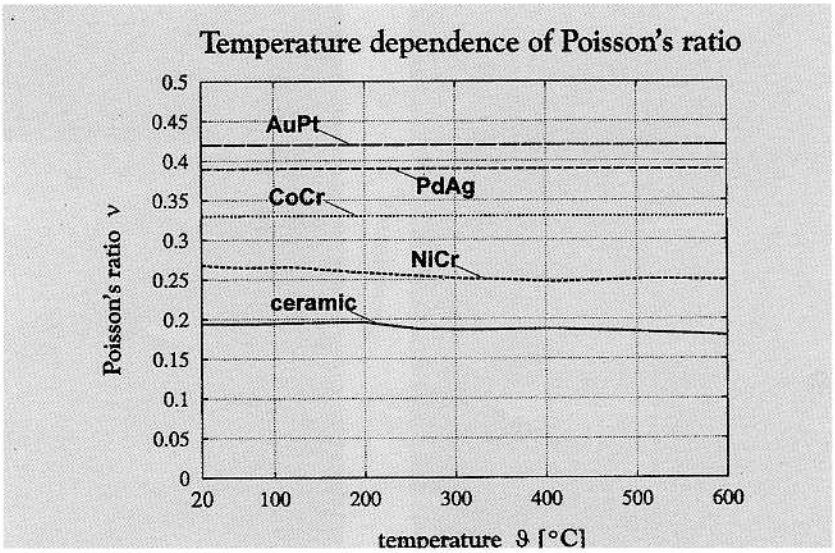

Fig 4 Temperature-dependence of the Poisson's ratii of different alloys, and of porcelain.

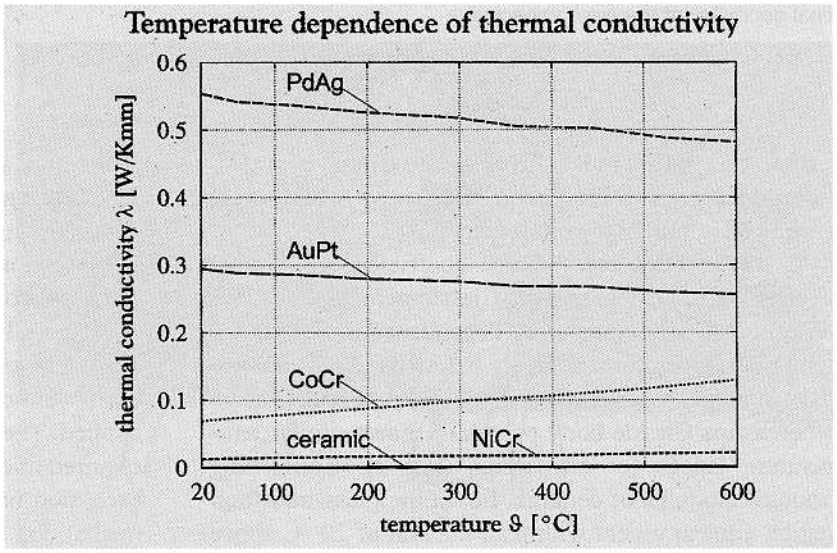

Fig 5 Temperature-dependence of the thermal conductivities of different alloys and of porcelain.

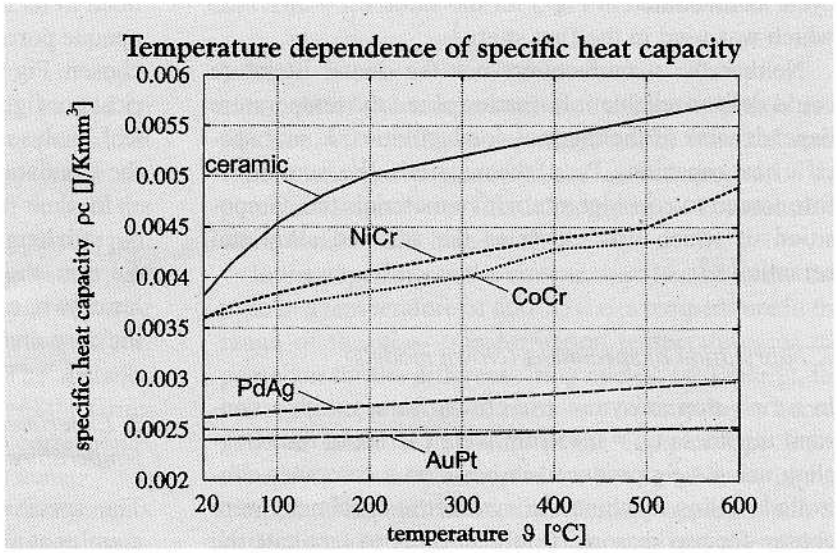

Fig 6 Temperature-dependence of the specific heat capacities of different alloys, and of porcelain.

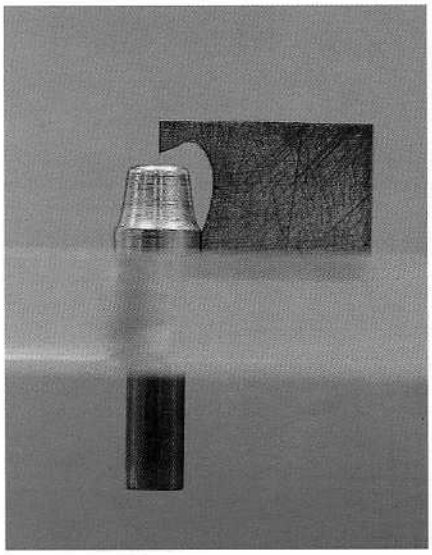

Fig 7 Stripping blade used to achieve the final geometry of the crown specimen.

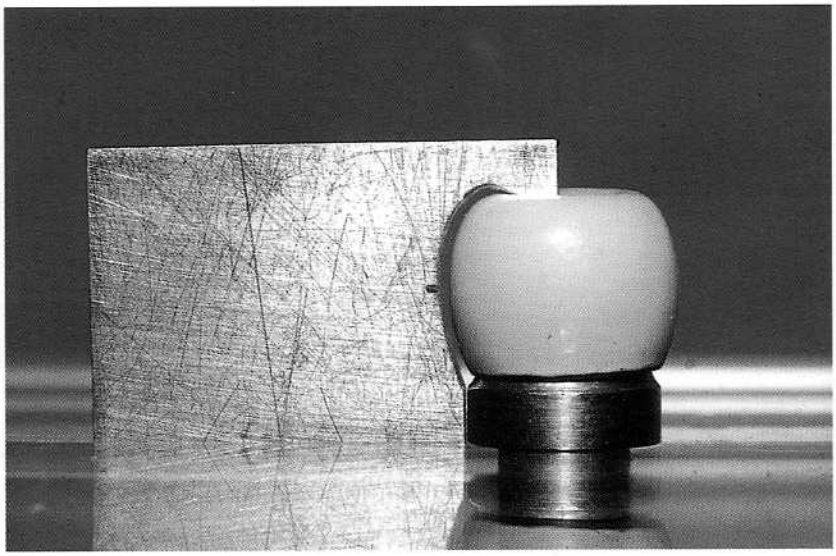

Fig 8 Crown specimen after the third firing.

many) and a CoCr-alloy (Remanium 2000; manufacturer: Dentaurum, Pforzheim, Germany) which were employed in our first experiment.[1]

It should be noted that the coefficient of thermal expansion, α_C, of opaque ips-Classic porcelain displays an "anomalous" temperature dependence in the second firing at temperatures scarcely below its glass-transformation point as compared with the other firings (Fig 1), whereas ips-Classic body porcelain shows similar temperature lapses for all firings (Fig 2). Concerning Young's modulus of ceramic, Ec, in the glass-transition region a linear ascent within an interval of 20 °C above the value ϑ_G in question was assumed in each firing cycle as illustrated in Fig 3 for the value ϑ_G = 581.7 °C which was used in the first study.[1]

Neither the manufacturers nor the dental literature could deliver reliable information about the temperature dependencies of the thermal conductivities, λ, and specific heat capacities, Pc, of the materials. We were therefore forced to consider alternative materials the composition of which was closer to the selected alloy and ceramic.[7,8,9]

2. Fabrication of specimens (crown models)

In a first step axisymmetric crown frames with a constant thickness t_M = 0.45 mm were cast from the NiCr-alloy using a jig produced in brass on a computer-controlled milling machine. Axisymmetric specimens were chosen for two reasons: firstly, in order to facilitate the fabrication of consistently identical crown specimens; secondly, and fundamentally, because the experimental determination of surface temperature distribution for a *non*-axisymmetric crown required a much larger number of thermocouples.

A special device was constructed to allow rotation of the specimens (n = 5) against fixed stripping blades in each step of manufacture, after porcelain had been applied. These blades had the desired external contours required in each firing step (the shrinkage of ceramic in each step had been determined in preliminary experiments). Fig 7 shows the stripping blade used to achieve the final form of the crown. Fig 8 presents such a specimen in its final form, i.e. after the last firing cycle. For opaque porcelain a constant thickness t_O = 0.20 mm was chosen. Fig 9 schematically illustrates the three geometrical configurations used in the experiments and numerical analyses (the last configuration being identical to the simulation of the glazing process).

In their final configuration the specimens had an overall height of 7.5 mm and a maximum radius of 4.1 mm, thus approximately corresponding to a premolar crown, as they also did in regard to the geometry of the cusp and the margin.

3. Experimental determination of the surface temperature distribution

The specimens were equipped with NiCr/Ni-thermocouples at a series of points on the outer ceramic veneer

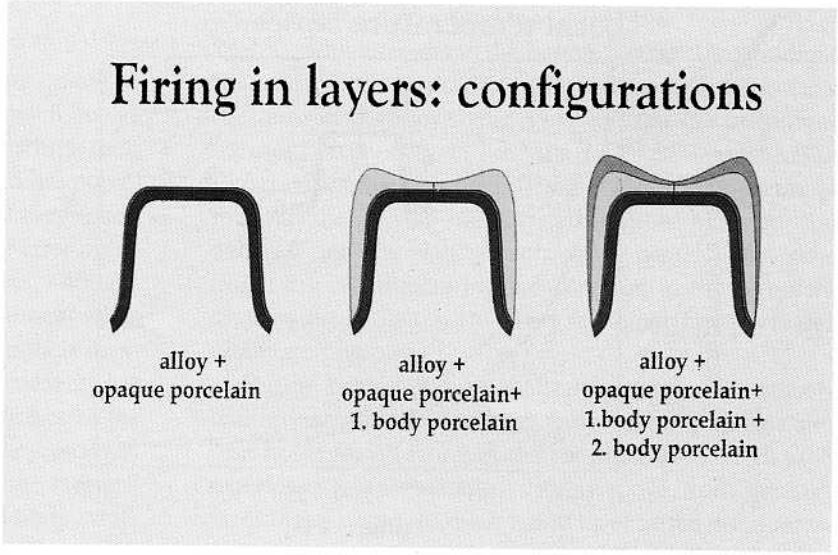

Fig 9 Scheme of the geometrical configurations (opaque layer, first dentin layer, final configuration) used in the experimental/numerical analyses.

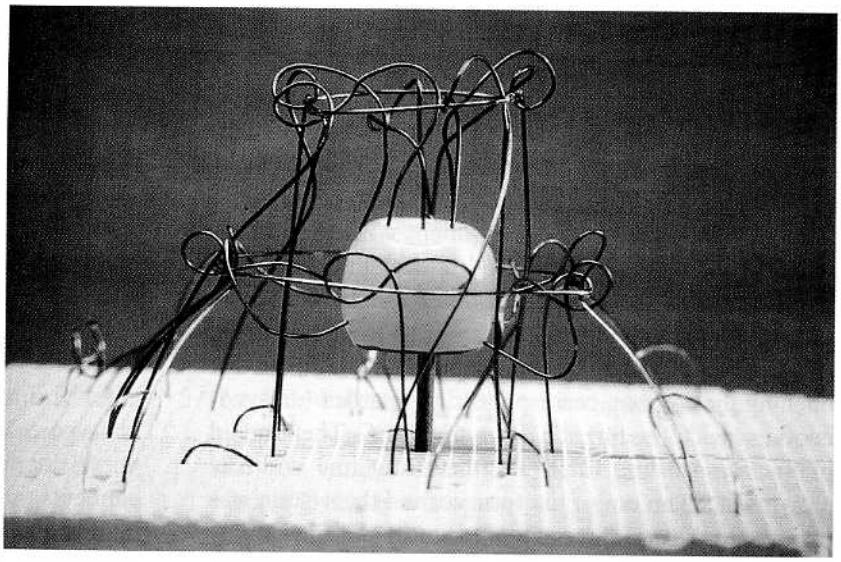

Fig 10 Crown specimen equipped with thermocouples, mounted on the firing support.

and the inner alloy frame, these points being located on the contour of an intersection through the crown which marked the symmetrical axis. On the alloy frame the thermocouples were lasered to the surface so that the central (axial) thermocouple served as a supporting pin. In order to achieve contact with the ceramic veneer, the thermocouples were fastened to a surrounding wire cage, thus allowing their resilient support on the surface. Fig 10 illustrates such an arrangement. The distance between the crown's margin and the surface of the firing support (tray) was adjusted to 6 mm, which corresponds approximately to that of commercial pin systems.

The electronic equipment (National Instruments SCXI-1000, 1100, 1300) permitted a *simultaneous* measurement of the temperature in the contact points as a function of cooling time, whereby the start of each experiment was triggered at the instant the lid of the porcelain furnace was lifted (Programat P 90; manufacturer: Ivoclar, Liechtenstein).

In the experiments the crowns were heated in the furnace to a temperature of 600 °C (i.e. a temperature in the range of the glass-transformation temperatures of the porcelain for the different firing cycles; cf. Table 1), the halting time of about 12 minutes guaranteeing a homogeneous initial temperature in the complete specimen. (The NiCr/Ni-thermocouples are not suitable for higher temperatures, and alternative thermocouples made to withstand greater heat could not be used because of their

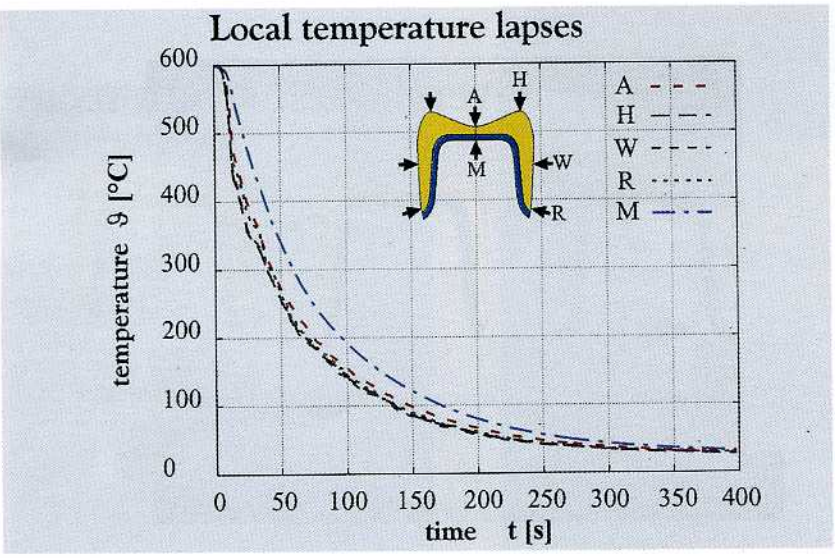

Fig 11 Typical temperature lapses at four control points on the veneer and at the central point of the frame in the final configuration (third firing).

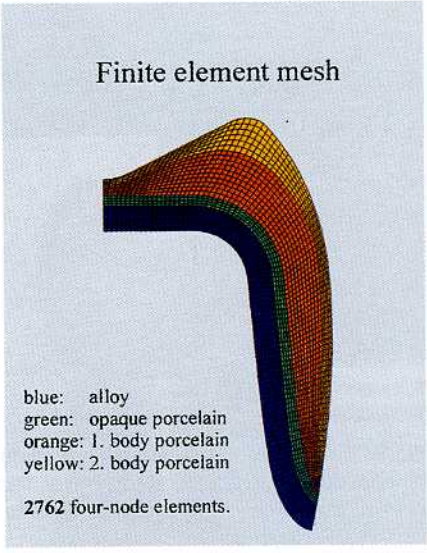

Fig 12 Finite element mesh with 2762 four-node elements used in the simulation of the third firing and and the fourth firing (glazing).

distinctly larger cross-section which, with tiny specimens, could possibly have led to a heat flux falsifying the true local temperature.) In this respect the cooling process simulated in the experiments, from the firing temperature down to the temperature at the instant of opening the furnace, corresponded to retarded (delayed) cooling inside the furnace down to 600 °C. Then the lid of the furnace was lifted off, the firing tray with the crown was taken out of the furnace, and the system was exposed to the air (at room temperature) and shielded by a wide cylinder to avoid the uncontrolled flow of air. Fig 11 shows the recordings of typical temperature lapses at four control points on the veneer and the central point on the alloy frame in the final configuration (third firing).

For each specimen the measurements were repeated ten times for statistical reasons. Finally the mean local temperature values as a function of time were determined from all these measurements of all the specimens. The maximum standard deviations were < 4 % across the entire cooling interval from 600 °C to 20 °C.

4. Numerical procedure (Finite Element Method)

The temperature lapses measured at the discrete surface points were smoothed numerically to a continuous, time-dependent surface temperature distribution. This was used as input to a finite element (FE) analysis carried out with ANSYS 5.3 to compute the temperature distribution in the interior of the crown and, finally, the distribution of thermal stresses in the system, both as functions of time. The mesh used consisted of 1200 (first firing: opaque porcelain), 2219 (second firing: body porcelain) and 2762 (third correction firing: body porcelain; fourth firing: glazing; cf. Fig 12) four-node elements, respectively. Analyses prior to the final calculations confirmed that a further refinement of the mesh resulted in negligible discrepancies. The following flow chart illustrates the experimental-numerical procedure employed:

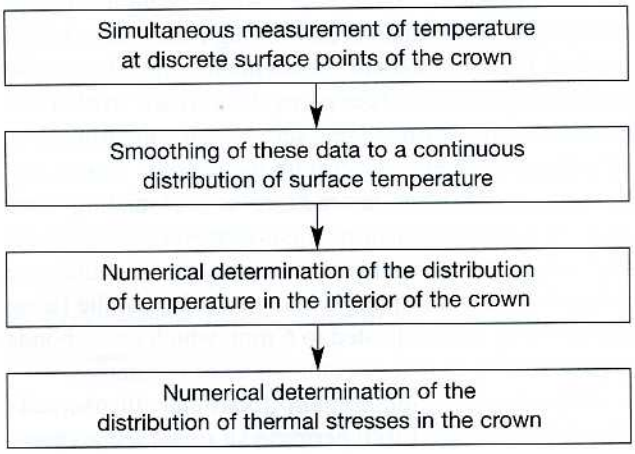

Results

In all four firing cycles the frame possesses a practically homogeneous temperature distribution in each instant of the cooling phase due to the comparatively high thermal conductivity of the alloy as compared to the porcelain. It is also typical of all firing cycles that the highest transient stresses in the veneer occur shortly after opening the porcelain furnace (i.e. within the first ~ 40 seconds). They occur practically at the same moment when the temperature gradients in the veneer reach their maximum. The highest temperatures are always measured at the surface of the veneer, the lowest at the surface of the frame, and these temperature differences can considerably exceed 100 °C. This disparity is due to the fact that the veneer can freely radiate heat into the vicinity while the surface elements of the frame are essentially radiating at each other (quasi radiation equilibrium), and that, via free convection, passing air can withdraw much more heat from the surface of the veneer than from the interior of the crown, which forms a cavity (stated simply, radiation dominates at high and convection at lower temperatures). This explains the development of the temperature distribution found in the simulations. Immediately after opening the furnace, temperature gradients build up in the porcelain which grow monotonically with time until a maximum is reached, which is followed by a monotonic decrease of the gradients down to room temperature.

In the following series of figures we present, for each firing cycle, the distribution of maximum *transient* stresses in the ceramic veneer (i.e. only for that part of the crown which is most likely to be exposed to failure) along with the pertinent temperature distribution in the *complete* crown, and the distribution of *residual* stresses in the veneer, restricting ourselves to half cross-sections. The *maximum principal stress* is used as a stress measure (positive values denote tension, negative values pressure) in view of the fact that ceramic, as a brittle material, is especially sensitive to tensile stresses. The figures contain at the top, in white, the moment t (in seconds: s) after opening the furnace (at time t = 0), and in the lower right corner, in blue the lowest, in red the highest instantaneous temperature (in °C) or stress (in MPa) value, respectively. A fine graduation of the corresponding values can be gathered from the color scale in the upper right corner.

In the following the time at which the maximum transient stresses occur is denoted by t*.

Figs 13a, b present the temperature and stress distribution for the first (opaque) firing at time t* = 16 s. The temperature difference between the surface of the veneer and the frame then amounts to $\Delta\vartheta \approx 498\ °C - 350\ °C = 148\ °C$, which results in the largest temperature gradient recorded during the complete fabrication process (because of the thin layer). This leads to the maximum transient stress $\sigma = 114.8$ MPa (also the largest value found during the complete firing cycle) which occurs at the surface in the transitional region between the occlusal and the wall section of the crown. The additional Fig 14, illustrating the situation in the *complete* system, shows that at t* = 16 s the alloy frame is under moderate pressure.

During further cooling the transient stresses gradually diminish due to decreasing temperature gradients and (this holds for *all* firing cycles) at times $t \approx 80–110$ s the maximum thermal stresses finally move from the surface of the veneer to the opaque layer at the bond interface, and to the curved transitional region between the occlusal and the wall sections. These transient "bond" stresses increase during cooling time. About 950 s after opening the furnace the system is practically cooled down to room temperature, 20 °C (temperature variations ≤ 1 °C), and the crown is set under the final residual stress distribution.

This residual stress distribution in the opaque layer is shown in Fig 15. The maximum tensile residual stress at the bond interface is given as $\sigma = 14.4$ MPa. Altogether the layer is set under pressure (central and marginal region) or at most moderate tension. As an overview Fig 16 presents the situation in the complete system which shows that high stresses up to $\sigma = 92$ MPa exist in the frame in the vicinity of the crown's margin.

In the second firing cycle (first layer of body porcelain) the temperature difference at time t* = 18 s (Fig 17a) is given as $\Delta\vartheta \approx 516\ °C–393\ °C = 123\ °C$. (The slight lacing of the crown's surface near the margin was introduced to avoid stress concentration due to a sharp edge during the following firing process.) The pertinent maximum transient stress in the veneer amounts to $\sigma = 53.5$ MPa (Fig 17b), occurring in the neighborhood of the cusp. Fig 18 illustrates the distribution of residual thermal stresses in the veneer: the maximum value amounting to $\sigma = 54.8$ MPa is again found at the material interface in the transitional region between the occlusal and the wall sections of the crown.

During the third firing cycle (correction firing of body porcelain) the temperature difference at time t* = 40 s (Fig 19a) amounts to $\Delta\vartheta \approx 389\ °C–273\ °C = 116\ °C$. The maximum transient stress in the veneer reaches the value $\sigma = 54.6$ MPa at the surface of the wall section (Fig 19b), i.e. about the same value as in the preceding firing cycle. The maximum residual stress, however, given as $\sigma = 76.5$ MPa and again occurring at the

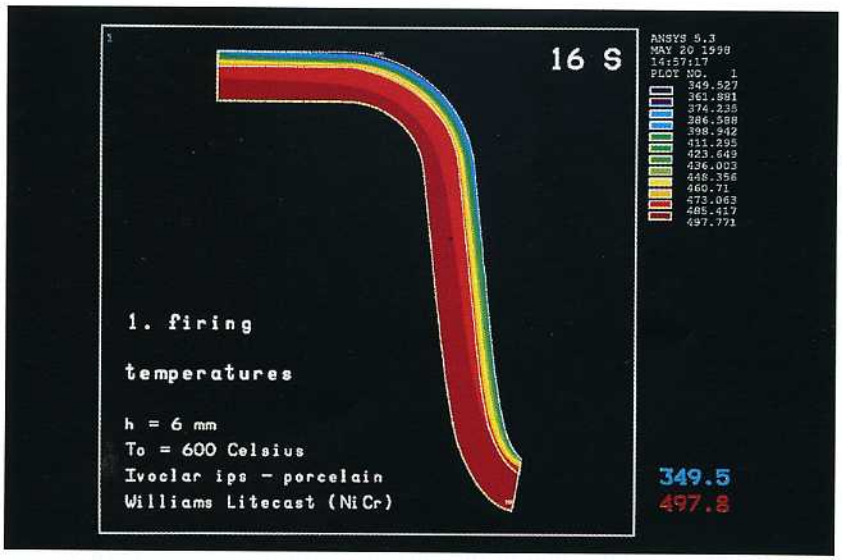

Fig 13a Temperature distribution in the complete crown for the first (opaque) firing 16 seconds after opening the furnace.

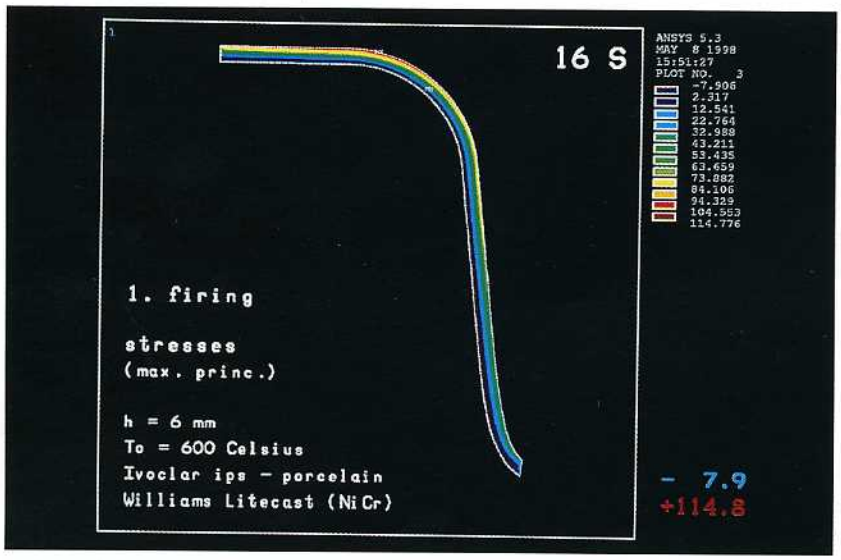

Fig 13b Accompanying distribution of transient stresses in the ceramic veneer.

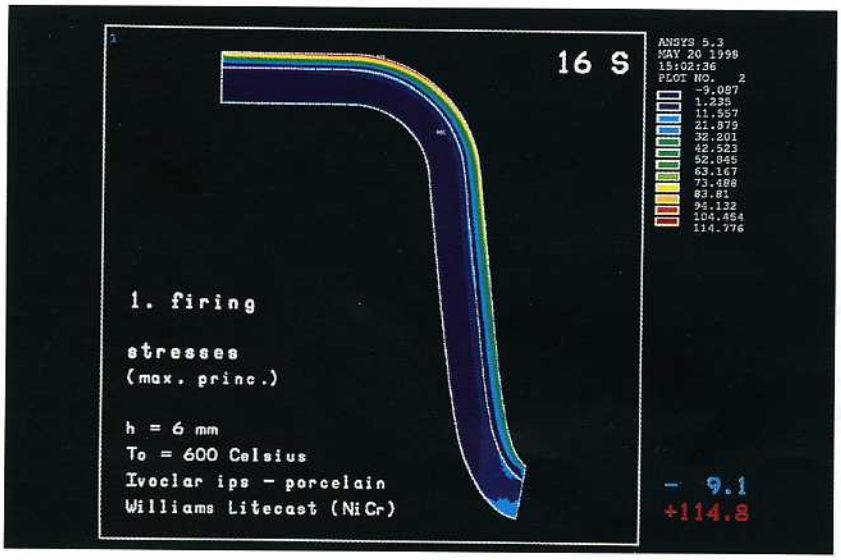

Fig 14 Distribution of transient stresses in the complete crown for the first (opaque) firing 16 seconds after opening the furnace.

Fig 15 Distribution of residual stresses in the opaque layer.

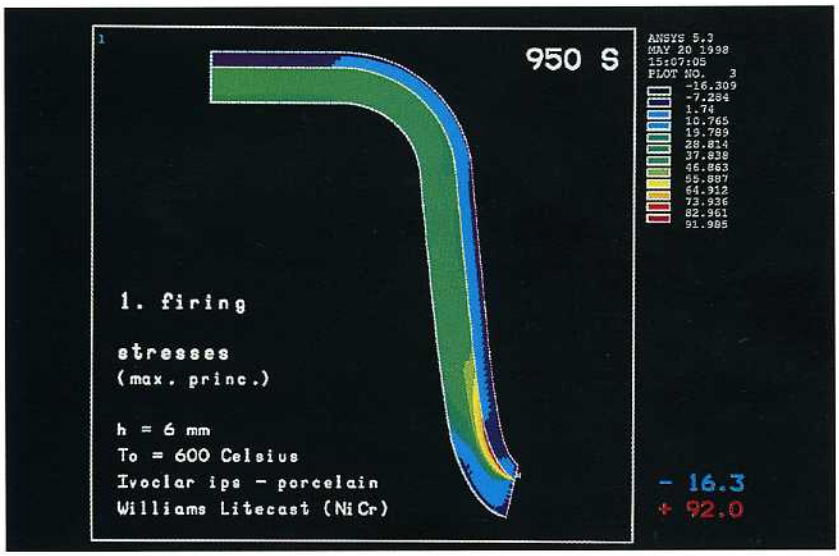

Fig 16 Distribution of residual stresses in the complete crown.

Fig 17a Temperature distribution in the complete crown for the second (first dentin) firing 18 seconds after opening the furnace.

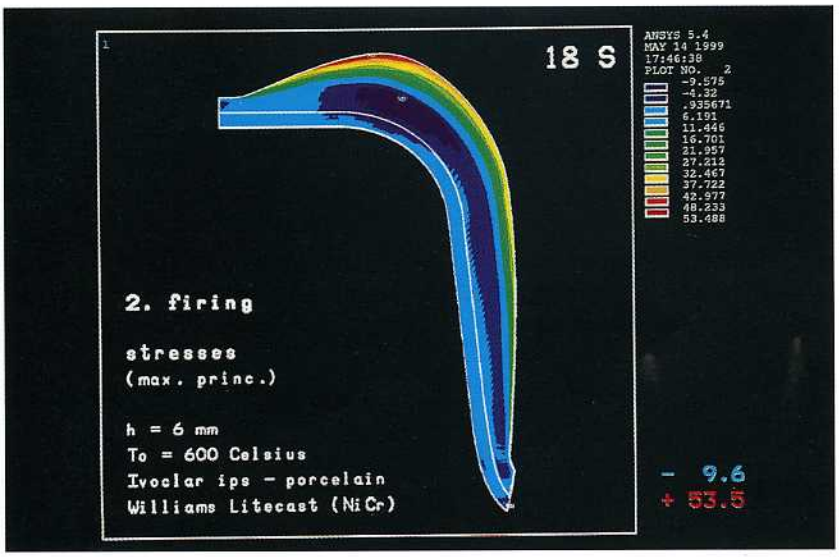

Fig 17b Accompanying distribution of transient stresses in the ceramic veneer.

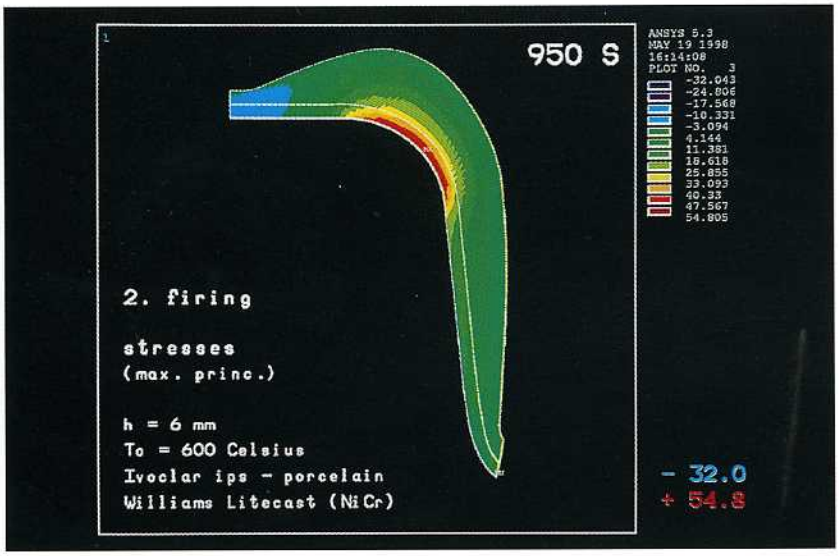

Fig 18 Distribution of residual stresses in the veneer after the second firing.

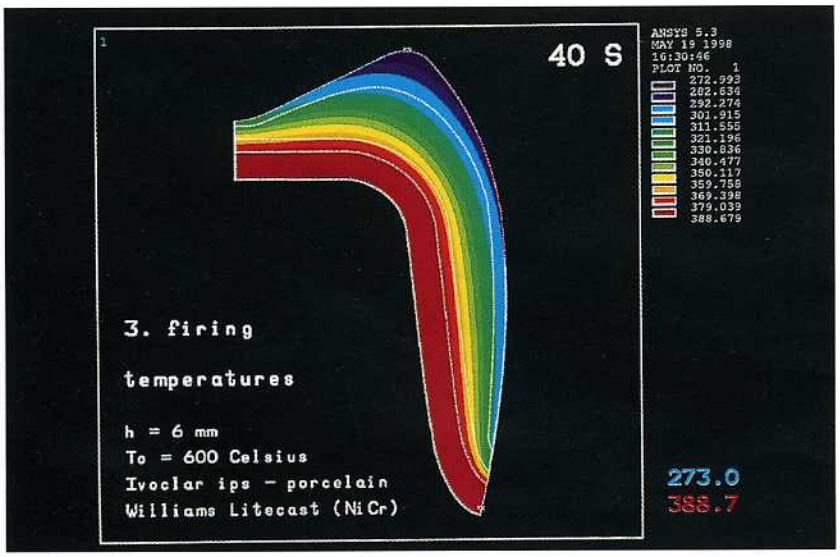

Fig 19a Temperature distribution in the complete crown for the third (dentin correction) firing 40 seconds after opening the furnace.

Fig 19b Accompanying distribution of transient stresses in the ceramic veneer.

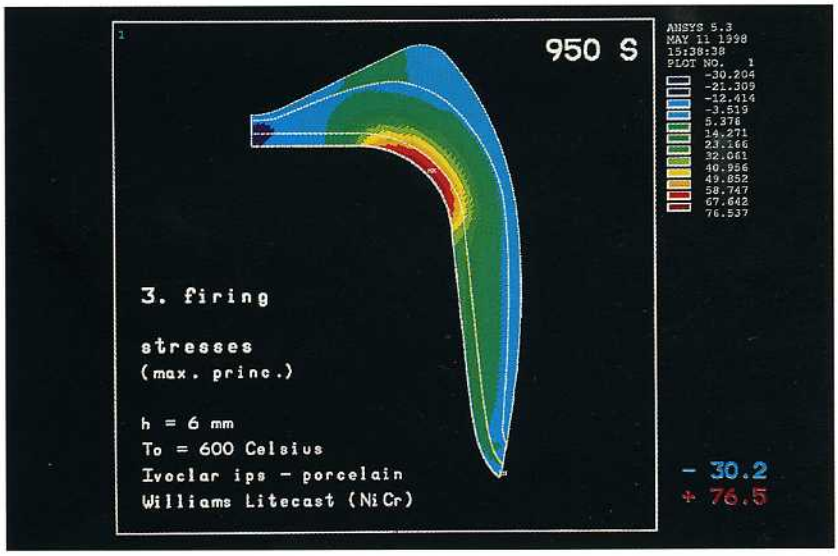

Fig 20 Distribution of residual stresses in the veneer after the third firing.

material interface in the transitional region between the occlusal and the wall sections of the crown, has risen dramatically (Fig 20).

Finally, during the fourth firing cycle (glazing), at time $t^* = 24$ s when $\Delta\vartheta \approx 482$ °C–361 °C = 121 °C, the maximum transient stress amounts to $\sigma = 41$ MPa (Figs 21a, b) and occurs at the surface of the cusp. The final residual stress distribution in the ceramic veneer is shown in Fig 22: the surface of the veneer is set under pressure or moderate tension, respectively, whereas the opaque porcelain is again loaded with high tensile stresses at the bond interface, the maximum amounting to $\sigma = 74.7$ MPa. As an overview the residual stress distribution in the *complete* crown is presented in Fig 23. It becomes obvious that in the central part of the frame high tensile stresses up to $\sigma = 239.6$ MPa are "frozen in" whereas its marginal region is essentially not under pressure.

Table 2 shows the results obtained in the four simulated firing processes.

It should be noted that the *residual* thermal stresses can be calculated directly from the values E_M and E_C, ν_M and ν_C, α_M and α_C, and ϑ_G, irrespective of the special cooling history. These values differ less than 0.5 % from those obtained at $t = 950$ s.

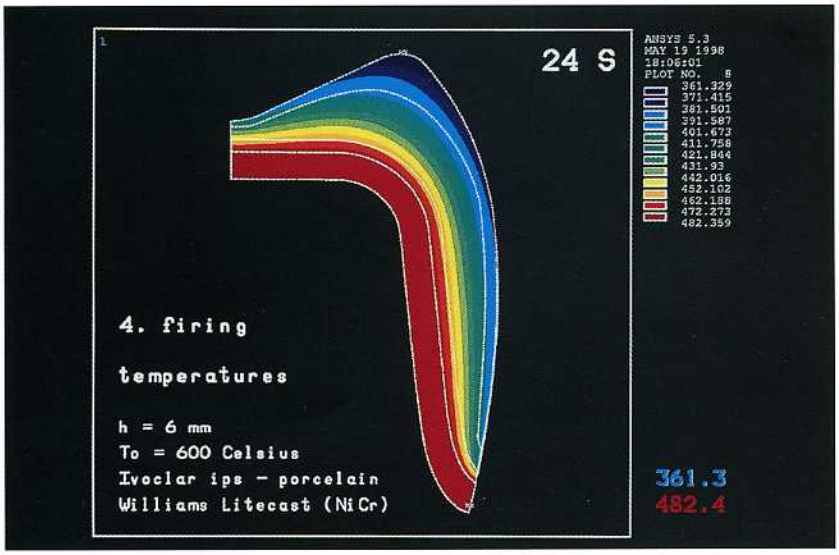

Fig 21a Temperature distribution in the complete crown for the fourth firing (glazing) 24 seconds after opening the furnace.

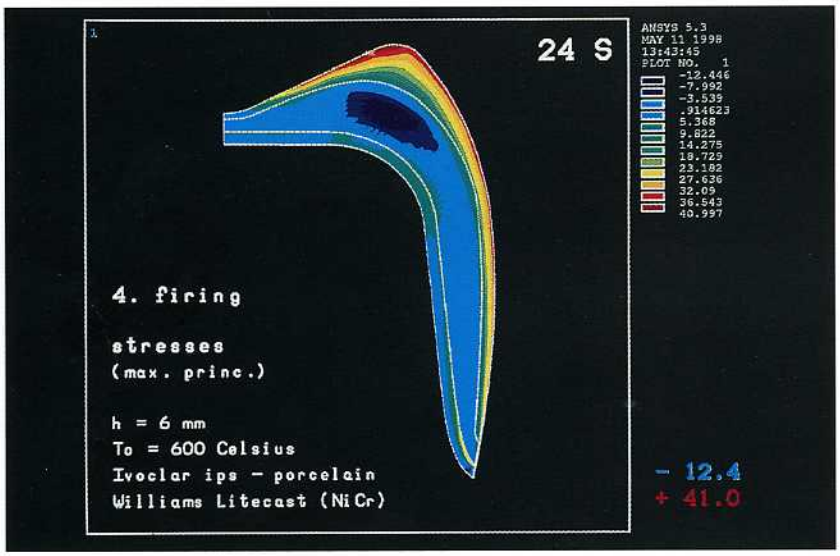

Fig 21b Accompanying distribution of transient stresses in the ceramic veneer.

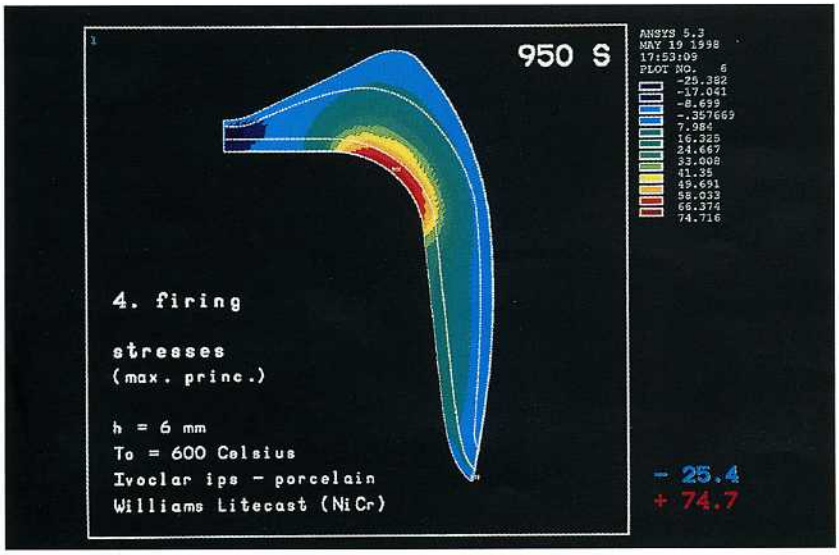

Fig 22 Distribution of residual stresses in the veneer after the fourth firing (glazing).

Fig 23 Distribution of residual stresses in the complete crown after glazing, i.e. the stress state "frozen in" after completion of the fabrication process.

TABLE 2 Maximum transient and residual thermal stresses occurring during the four firing cycles

	Maximum transient principal stress [MPa] (at time t*)		Maximum residual principal stress [MPa]
1st firing: opaque porcelain	114.8	(16 s)	14.4
2nd firing: opaque + body porcelain	53.5	(18 s)	54.8
3rd (correction) firing: opaque + body porcelain	54.6	(40 s)	76.5
4th firing: glazing	41.0	(24 s)	74.7

Discussion

For the considered material combination, Williams Litecast/ips-Classic porcelain, the simulation of the development of thermal stresses during the four firing cycles shows that the maximum transient and the maximum residual stresses in the ceramic veneer are essentially of the same magnitude. These stresses were calculated under the assumption that both materials, alloy and porcelain, can be modeled as linear-elastic materials, i.e. the possible viscoelastic behavior of porcelain at high temperatures, and thus stress relaxation, has not been taken into account. Therefore, the presented stress values are most likely somewhat higher than in reality. Nevertheless, the presented values allow a comparison of the stresses during the different firing cycles.

In the 1999 study[1] the authors presented a simplified model simulating the firing of the complete veneer all at once (the "single layer" simulation). In that paper the (mean) coefficients of thermal expansion, as stated by the manufacturers, were set at $\alpha_M = 14.4 \times 10^{-6}\ K^{-1}$ for the NiCr-alloy and at $\alpha_C = 12.8 \times 10^{-6}\ K^{-1}$ for ips-Classic porcelain (approximately corresponding to the mean value of the body porcelain for the first three firings, as listed in Table 1) in the interval between glass-transformation temperature $\vartheta_G = 581.7$ °C and room temperature $\vartheta_R = 20$ °C. The temperature dependence of α_C resembled that of Fig 3 for the third firing; the temperature dependence of α_M was the same as here. The main result was that the maximum transient stress in the veneer ($\sigma \approx 68$ MPa) was much higher than the maximum residual stress ($\sigma \approx 40$ MPa).

However, with the exception of the first (opaque) firing, this more realistic investigation of firing in layers shows an inversion of this relationship: the maximum transient stresses are seen to be of the same magnitude

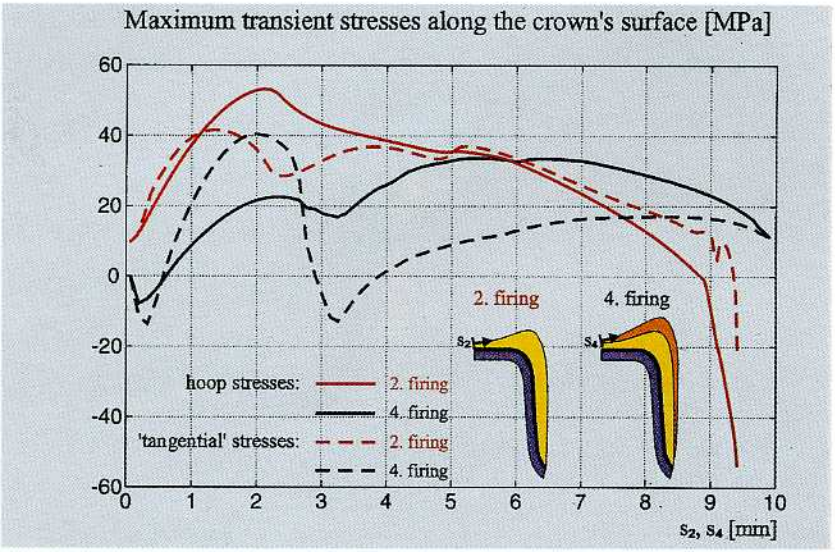

Fig 24 Distribution of transient hoop and tangential stresses at the surface of the crown during the second firing and fourth firing (glazing) 18 and 24 seconds, respectively, after opening the porcelain furnace. Coordinate s measures the distance of a surface point from the symmetrical axis along the surface contour.

(in the second firing) or considerably lower (in the third and fourth firings) than the maximum residual stresses (cf. Table 2).

For the considered material combination the maximum transient stresses in porcelain have a tendency to decrease with each firing whereas the maximum residual stresses increase. Glazing delivers a considerable relief of the transient stresses, but leaves the residual stresses practically unchanged.

To obtain a more detailed insight into the stress distribution at the critical loci of the crown, we also analyzed the *maximum transient stresses* along the surface of the crown at time t = t* (t* = the instant of occurrence of maximum transient stresses), and the *residual normal and shear stresses* along the bond contour.

Since the crown is free from tractions, an area in the tangential plane (the surface element) is stress-free and the principal direction is from the normal to the surface. For the two remaining perpendicular areas on the surface of the crown Fig 24 shows the lapse of pertinent normal transient stresses σ_1 and σ_2 as a function of the coordinate s (arc length), measuring the distance of a surface point from the symmetrical axis along the surface contour.

Here σ_1 denotes the *hoop stress*, i.e. the normal stress in an area of a cross section through the crown containing its symmetrical axis, whereas σ_2 denotes the normal stress in an area perpendicular to the crown's surface contour, which is always directed tangentially towards the surface contour (in what follows this stress component is referred to as *tangential stress*). Fig 24 shows these stresses for the second firing (i.e. at time t* = 18 s) as a function of the arc length s_2, and for the fourth firing (i.e. at time t* = 24 s) as a function of the (modified) arc length s_4.

In the second firing (red curves) both surface stresses are tensile throughout with the exception of a small region near the margin of the crown. The maximum hoop stress occurs near the top of the cusp and amounts to $\sigma_{1,max}$ = 53.5 MPa (maximum transient stress; cf. Table 2). This stress is greater than the maximum tangential stress $\sigma_{2,max}$ = 41.5 MPa occurring between the symmetrical axis and the cusp. The maximum compressive hoop stress and tangential stress at the marginal end of the veneer are given as $\sigma_{1,min}$ = 54.0 MPa and $\sigma_{2,min}$ = –20.8 MPa respectively.

During glazing (the fourth firing) the highest transient stress is the tangential stress near the top of the cusp, which amounts to $\sigma_{2,max}$ = 41.0 MPa (maximum transient stress; cf. Table 2). Now the maximum hoop stress occurring in the central wall section, which has the value $\sigma_{1,max}$ = 33.5 MPa, is smaller than the maximum tangential stress. Both stresses are compressive in the vicinity of the symmetrical axis and the tangential stress again assumes negative values in the transitional region between the cusp and the wall of the crown (the magnitude of these compressive stresses is less than 13 MPa, however, thus being considerably smaller than the tensile stresses).

Since porcelain, a typically brittle material, is especially sensitive to tensile stresses, transient stresses in the cusp region and central part of the wall may lead to surface cracks.

Fig 25 shows the lapse of normal and shear residual stresses along the bond interface contour (coordinate s*) after the second and fourth firings. The *shear* stresses

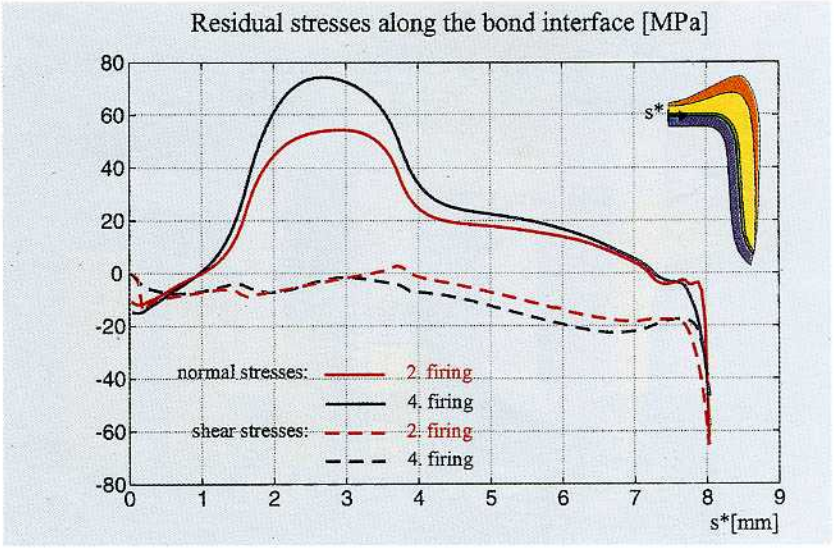

Fig 25 Distribution of normal and shear residual stress along the bond interface for the second and fourth firings, respectively; coordinate s* measures the distance of a point on the bond interface from the symmetrical axis along the bond contour.

are essentially negative and of moderate magnitude throughout, though there is a sudden (negative) increase near the margin of the crown (i.e. high shear stresses at the bond interface in the marginal zone of the veneer). These highest values are given as $\sigma_{shear} = -65.2$ MPa (second firing) and $\sigma_{shear} = -46.8$ MPa (glazing). The *normal* stresses are essentially tensile, except in the vicinity of the symmetrical axis and the margin, and reach their maximum values in the transitional region between the occlusal and wall sections of the crown. These maximum values are given as $\sigma_{normal} = 54.4$ MPa (second firing) and $\sigma_{normal} = 74.1$ MPa (glazing). The maximum normal compressive stresses at the margin are $\sigma_{normal} = -61.8$ MPa (second firing) and $\sigma_{normal} = -51.9$ MPa (glazing).

Evidently the regions of the bond interface with the highest risk of debonding are the transitional zone between the occlusal and wall sections (where there are high tensile stresses) and the marginal region of the crown (where there are high shear stresses). It should be noted, however, that the high shear stresses near the margin of the crown are "buffered" by normal *compressive* stresses of about the same magnitude (i.e. the frame and the veneer are pressed together), which partially neutralizes the debonding effect of the shear stresses. It may therefore be expected that the curved section of the bond interface, exposed to high tensile stresses, is more likely to fail.

In the literature[9,10] the values $R_m \approx (25–40)$ MPa for the tensile strength of porcelain and $\sigma_b \approx (65–125)$ MPa for its bending strength, each at room temperature, can be found. Strength values at high temperatures are, however, not known to the authors. Compared with these data, especially as regards the tensile strength, the maximum principal stresses presented in this investigation are for the most part already in the critical range. There is, however, no constant tensile stress, transmitted across the complete cross section as in the tensile test, in the crown. Flexure strength is therefore seen to be a more realistic measure of the risk of cracks, spallations, etc. However, it is clear from the results shown in Table 2 and Fig 24 that the calculated flexure stress values come close to, or within, the critical range (but note that stress relaxation due to the possible viscoelastic behavior of ceramic at high temperatures has not been included in our model). Nevertheless, during the fabrication of the crown specimens failure was never observed.

With regard to the risk of debonding we have to compare the stresses calculated at the material interface (cf. Fig 25) with corresponding metal-ceramic bond strength values. In the ISO test (the three-point flexure bond test), where the geometry of the test specimen determined that the shear and normal stresses at the endangered site were of the same magnitude,[11] bond strengths in the range $\tau_b \approx (30–65)$ MPa were measured. Thus the stresses observed along the bond interface also fall partly into the critical range. It is evident from Fig 24 that the transitional region between the occlusal and wall sections of the bond interface, as well as its marginal zone, are especially in danger of debonding. However, no damage to the bond was registered in the fabrication of the crown models.

In this context we should like to mention an interesting result already obtained in our "single layer" simulation study. It is known from continuum mechanics that stress concentrations exist at sites of a loaded body

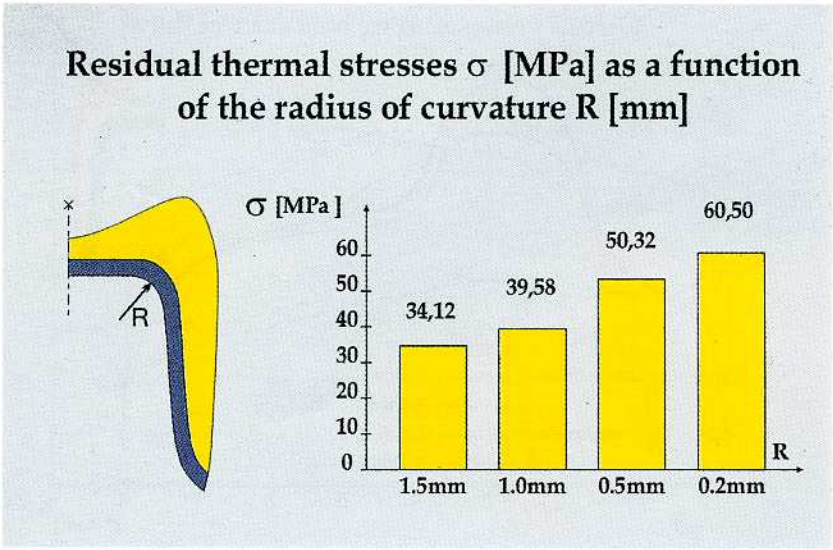

Fig 26 Maximum residual stress (at the center of the bond interface in the transitional region from the occlusal to the wall section of the crown) as a function of the (interior) radius of curvature ("single layer" simulation).

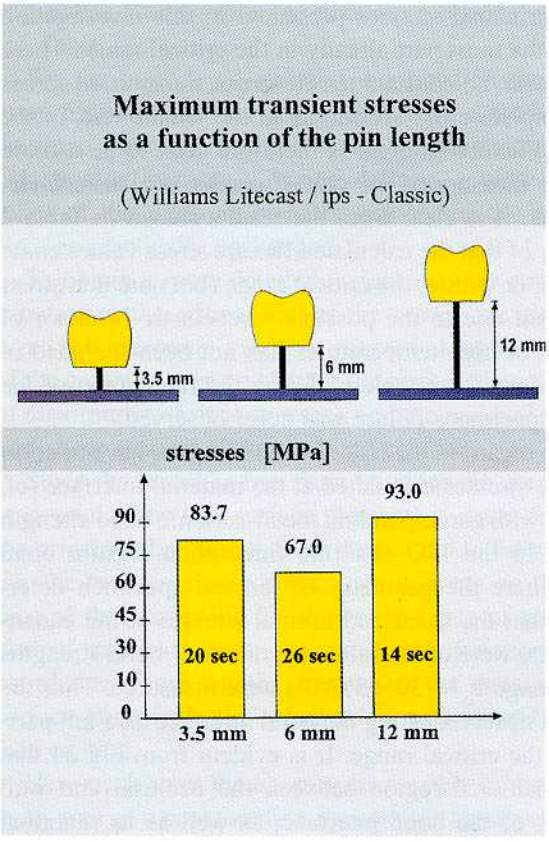

Fig 27 Dependence of the maximum transient stresses on pin length, i.e. the distance between the margin of the crown and the firing support ("single layer" simulation).

where small radii of curvature occur. To elucidate this fact *quantitatively,* Fig 26[1] shows the maximum principal residual stress in the center of the curved region of the bond interface as a function of the (interior) radius of curvature, R (to get the radius of curvature of the bond interface itself, the frame thickness of 0.45 mm has to be added to R), given as R = 1 mm in the present paper. It is clear that the bond stresses increase dramatically with the decreasing of radius R. The dental technician should therefore try to exclude loci with small radii of curvature (brims, edges etc.) from the bond surface. The dentist himself can contribute to a geometrically advantageous configuration by the appropriate preparation of the abutment tooth.

Further investigations in our earlier study[1] proved that the maximum transient stresses during cooling depended in a surprising way on the distance between the margin of the crown and the firing support, determined by the length of the pins used. In the results presented here this height was chosen as h = 6 mm which corresponds approximately to most commercial pin systems. Smaller (h = 3.5 mm) and greater distances (h = 12 mm) both delivered higher stresses (Fig 27). The reason for this phenomenon has not yet been fully explored. Schlieren-optical's investigations made clear, however, that the convection flow patterns around the crown differ considerably for the three heights. Furthermore, it is conceivable that the distance h may play a dominant role in heat radiation.

Whereas the *residual* stresses are completely determined by the values of the material constants just mentioned, and by the specific geometry of the crown, the

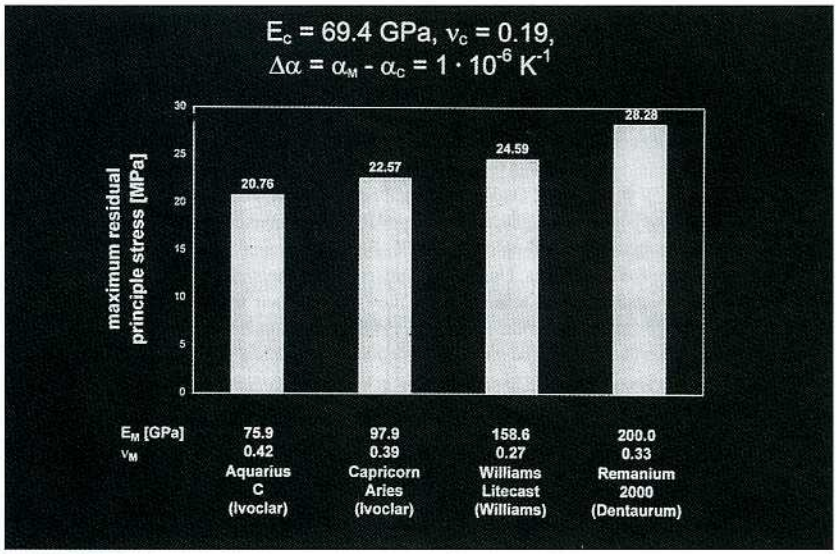

Fig 28 Dependence of the maximum residual principle stress on Young's modulus of the the alloy.

transient stresses can be manipulated by the cooling process. It is clear that a decrease of these stresses can be achieved by a reduction of the temperature gradients. In our previous study[1] it was shown that a lowering of the opening temperature of the furnace from 600 °C to 450 °C resulted in a reduction of ~30% in the maximum transient stresses.

Conclusions

This investigation shows that the thermal stresses in PFM restorations depend on a large number of parameters, including material coefficients, the global and local geometry of the object, specific cooling processes, and more. In the authors' opinion, a reliable and commonly accepted definition of the thermal compatibility of metal-ceramic systems is unlikely to be achieved.

In practice it is important that an alloy be combined with a porcelain for which the difference ($\alpha_M - \alpha C$) of the materials' coefficients of thermal expansion (as dominant parameters) is not too large. According to the presented results and dental practice, an approximate upper limit should be given as $\Delta\alpha = \alpha_M - \alpha_C \approx 2 \times 10^{-6}$ K^{-1} if the remaining important parameters (e.g. geometry, the cooling process etc.) are adjusted in the way described above. This upper limit will, however, depend on the chosen alloy: Fig 28 presents, for the identical value $\Delta\alpha = 1 \times 10^{-6}$ K^{-1}, the maximum residual stresses as a function of Young's modulus of the alloy, E_M, as calculated in our single layer simulation experiment[1] for a precious (Aquarius C), a palladium-base (Capricorn Aries), a NiCr- (Williams Litecast), and a CoCr-alloy (Remanium 2000). The stresses in the veneer are higher when Young's modulus of the metal is larger (the effect of Poisson's ratio on the magnitude of the stresses is negligible as can be shown by a variation of this parameter). We conclude that the choice of a secure value $\Delta\alpha = \alpha_M - \alpha_C$ for a possible characterization of thermally compatible ceramometallic combinations would also have to take into account the type of alloy.

Transient stresses in the veneer could be reduced if porcelains with a low coefficient of thermal expansion at high temperatures were available. We would encourage porcelain manufacturers to develop dental ceramics which cover a wider (higher) range of the mean value of α_C in the cooling interval between glass transformation and room temperature, so that thermally compatible porcelains may be made available for alloys with a high α_M value (AuPtAg and AuPdAg-alloys). Finally, in most commercial ceramic systems the coefficient of thermal expansion of opaque porcelain is higher than that of body porcelain[10] (ips- Classic is an exception) although it is conceivable that in certain situations a reciprocal relationship would be more advantageous.[12]

In closing we note that only *one* alloy/porcelain combination was investigated in this work. It is possible that corresponding analyses with other dental ceramics, with deviating thermal behavior, might deliver quite different results.

Acknowledgements

The authors express their gratitude to the Deutsche Forschungsgemeinschaft for financial support of this research project (SCHW 307/5-1, 5-2, 5-3).
They also acknowledge the supply of materials and equipment by Ivoclar (Schaan, Liechtenstein) and Williams International (Amherst, NY).
They are obliged to H. Pelka and P. Gadinger (dental laboratory H. Pelka, Stutensee, Germany) for manufacturing the crown specimens. Furthermore, they want to express their thanks to Dr.-Ing. H. Schmieg and W. Wendler (Institute for Mechanics, University Karlsruhe) for their valuable assistance in the experimental setup. Finally, they express their gratitude to M. Pliefke for his cooperation in the experiments and numerical analyses.

References

1. Thies M, Lenz J, Schweizerhof K. Wärmespannungen in metallkeramischen Kronen: Eine experimentell-numerische Analyse (Thermal stresses in ceramometallic crowns: An Experimental-numerical analysis). Teamwork 1999;2:42–59.
2. Thies M, Lenz J, Schweizerhof K, Waschbuesch K. Zur thermischen Verträglichkeit von Titan und Titankeramiken (Thermal compatibility of titanium and titanium porcelains). Dentallabor 2000;XLV-II, 3:367–383.
3. DeHoff PH, Vontivillu SV, Wang Z, Anusavice KJ. Stress relaxation behavior of dental porcelains at high temperatures. Dent Mater 1994;10:178–184.
4. Dehoff PH, Anusavice KJ. Viscoelastic stress analysis of thermally compatible and incompatible metal-ceramic systems. Dent Mater 1998;14:237–245.
5. Kaese HR, Tesk JA. Elastic constants of three Ni-Cr dental alloys at room and elevated temperatures. Dent Mater 1986;5:289–293.
6. Kaese HR, Tesk JA, Case ED. Elastic constants of two dental porcelains. J Mater Sci 1985;20:524–531.
7. Landolt-Boernstein. Data and Functional Relationships in Science and Technology, Vol. IV/4a. Berlin: Springer, 1967.
8. Landolt-Boernstein. Data and Functional Relationships in Science and Technology, Vol. IV/4b. Berlin: Springer, 1972.
9. Thies M. Beanspruchung metallkeramischer Kronen durch Wärmeeinwirkung bei der Herstellung und durch Kaubelastung (Stresses in Ceramometallic Crowns Due to Thermal Effects During the Fabrication Process and Under Mastication) [PhD thesis]. Karlsruhe: Universitaet Karlsruhe, 1994.
10. Das Dental Vademekum, 5. ed. Koeln: Deutscher Ärzte-Verlag GmbH, 1995.
11. Lenz J, Schwarz S, Schwickerath H, Sperner F, Schaefer A. Bond strength of metal-ceramic systems in three-point flexure bond test. J Appl Biomat 1995,6:55–64.
12. Lenz J, Raabe M. Zur Abstimmung der Wärmeausdehnungskoeffizienten von Legierung, Dentin und Opaker (Adjustment of the coefficients of thermal expansion of alloy, body and opaque porcelain). Dentallabor 1998;XLVI,11:1795–1801. □